Geochemical Perspectives Letters

© 2022 The Authors
Published by the European Association of Geochemistry

Experiments reveal enrichment of ^{11}B in granitic melt resulting from tourmaline crystallisation

L. Cheng[1,2*], C. Zhang[2,3*], Y. Zhou[1], I. Horn[2], S. Weyer[2], F. Holtz[2]

OPEN ACCESS

https://doi.org/10.7185/geochemlet.2206

Abstract

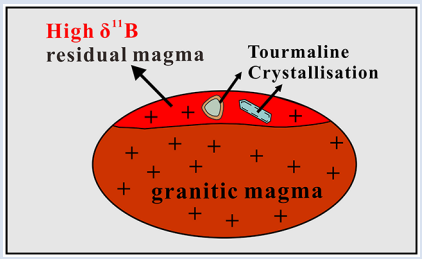

Tourmaline is the most common boron-rich mineral in magmatic systems. In this study, we determined experimentally the fractionation of boron isotopes between granitic melt and tourmaline for the first time. Our crystallisation experiments were performed using a boron-rich granitic glass ($B_2O_3 \approx 8$ wt. %) at 660–800 °C, 300 MPa, and $a_{H_2O} = 1$, in which tourmaline occurs as the only boron-hosting mineral. Our experimental results at four different temperatures show a small and temperature-dependent boron isotope fractionation between granitic melt and tourmaline ($\Delta^{11}B_{melt-Tur} = +0.90 \pm 0.05$ ‰ at 660 °C and $+0.23 \pm 0.12$ ‰ at 800 °C), and the temperature dependence can be defined as $\Delta^{11}B_{melt-Tur} = 4.51 \times (1000/T\ [K]) - 3.94$ ($R^2 = 0.96$). Using these boron isotope fractionation factors, tourmaline can serve as a tracer to quantitatively interpret boron isotopic ratios in evolved magmatic systems. Our observation that ^{11}B is enriched in granitic melt relative to tourmaline suggests that the $\delta^{11}B$ of late-magmatic tourmaline should be higher than tourmaline that crystallised at an early stage, if B isotope fractionation is not affected by other processes, such as fluid loss.

Received 27 August 2021 | Accepted 25 January 2022 | Published 24 February 2022

Introduction

Boron is an incompatible trace element that can be highly enriched in granitic melts and aqueous fluids (London *et al.*, 1996). The large difference in atomic mass by 10 % between the two stable isotopes of boron, ^{10}B and ^{11}B, results in significant variations in $\delta^{11}B$ of natural rocks that can be up to ca. 100 ‰. The separation of B-rich phases such as tourmaline and aqueous fluid from silicate melt is expected to produce B isotope fractionation due to the different B coordination (^{11}B at trigonal site and ^{10}B at tetrahedral site) in coexisting B-bearing phases (*e.g.*, Trumbull *et al.*, 2013; Siegel *et al.*, 2016). Thus, B isotopes are a sensitive tool to trace magmatic–hydrothermal processes (such as fractional crystallisation, degassing, ore formation) and metamorphic fluid source, and tourmaline, as the most common B-hosting mineral in granitic magma, can serve as a useful tracer for such processes. The negligible intra-crystalline diffusion rate leads to the consequence that B isotopic composition of tourmaline is not easily overprinted by late magmatic or hydrothermal events and therefore ideal to record the evolution history of magmas (*e.g.*, Marschall and Jiang, 2011). B isotope fractionation factors ($\Delta^{11}B_{melt-Tur}$) between silicate melt and tourmaline are a prerequisite to quantitatively interpret the B isotope composition of tourmaline in granitic systems. To our knowledge, so far, B isotope fractionation between granitic melt and tourmaline has not been directly determined by experiments. In previous studies (*e.g.*, Trumbull *et al.*, 2013; Siegel *et al.*, 2016), $\Delta^{11}B_{melt-Tur}$ values were indirectly calculated from the combination of experimental results on B isotope fractionation between hydrous melt and aqueous fluid ($\Delta^{11}B_{melt-fluid}$) (Hervig *et al.*, 2002; Maner and London, 2018) and between tourmaline and aqueous fluid ($\Delta^{11}B_{Tur-fluid}$) (Palmer *et al.*, 1992; Meyer *et al.*, 2008). However, these experimental studies differ in the experimental and analytical methods, the *P-T* conditions, and the fluid compositions. Such discrepancies can lead to great uncertainties if these experimental results are used to calculate $\Delta^{11}B_{melt-Tur}$ values. In addition, theoretical studies have suggested that the magnitude of $\Delta^{11}B_{Tur-fluid}$ depends on the composition of tourmaline, with a larger fractionation for dravite than for schorl (Li *et al.*, 2020), which further increases the uncertainty for indirectly calculated $\Delta^{11}B_{melt-Tur}$ values.

In this paper, we report results of tourmaline crystallisation experiments conducted for B-rich granitic systems in the temperature range of 660 to 800 °C and at 300 MPa. The analytical data of the B isotopic distribution between the experimental glasses and tourmalines provide direct constraints on the B isotope fractionation between granitic melt and tourmaline at magmatic temperatures.

Methods

Five tourmaline crystallisation experiments were performed at 660–800 °C, 300 MPa, $fO_2 \approx$ NNO for ~15–30 days in water-pressurised, cold-seal pressure vessels. A B-rich peraluminous granitic glass (B10 glass, $B_2O_3 \approx 8.8$ wt. %), which was synthesised by melting mixed powders of a B-free glass (BDG-1) and

1. State Key Laboratory of Earthquake Dynamics, Institute of Geology, China Earthquake Administration, 100029 Beijing, China
2. Institute of Mineralogy, Leibniz University Hannover, 30167, Hannover, Germany
3. State Key Laboratory of Continental Dynamics, Department of Geology, Northwest University, 710069 Xi'an, China
* Corresponding author (email: chenglining@ies.ac.cn; zhangchao@nwu.edu.cn)

boric acid powder, was used as starting material. Four water-saturated experiments ($a_{H_2O} = 1$) and one water-undersaturated experiment ($a_{H_2O} \approx 0.7$) were conducted. The activity of water was decreased by adding a fluid composed of mixed H_2O and CO_2 (added as silver oxalate). Major element compositions of the starting glass and experimental products were measured by electron microprobe analyser (EMPA) using a Cameca SX-100 microprobe. Boron isotope compositions of the starting glass and experimental products were measured in situ using a Thermo Scientific Neptune Plus, which was connected to a Spectra-Physics Solstice femtosecond laser ablation system. Details on the experimental and analytical methods are reported in Supplementary Information (SI).

Results

Experimental conditions and products are listed in Table 1. Tourmaline was observed in all experiments and homogeneously distributed in melts as dark-green euhedral and columnar crystals, with a common size of ~100 μm in length and ~50 μm in width (Fig. 1). In back-scattered electron (BSE) images, most tourmalines show a variation in darkness even within one crystal (Fig. 1b), and some grains are characterised by faceted hourglass sector zoning (see details in SI) (Fig. 1e, f). The Mg/[Mg + Fe] ratio is *ca.* 0.35–0.55 (Fig. S-2), which is typical for schorl and consistent with that of common igneous tourmalines in nature. Minor amounts of magnetite are evenly distributed in experiments. Bubbles were found in runs DC-28 and DC-87. Experimental melts (quenched as glasses) are peraluminous (ASI ≈ 1.1–1.4) and show a narrow range in B_2O_3 content (~7.7–8.0 wt. %). Additional details about experimental products and phase compositions are given in SI.

Boron isotopic compositions of the experimental tourmalines and glasses, as well as the calculated isotopic fractionation factors between them, are listed in Table 1. The starting glass (B10) shows a homogeneous B isotope composition within error, with $\delta^{11}B$ values of +0.92 ± 0.03 ‰ (Table S-5). The B isotope composition of experimental glasses ($\delta^{11}B_{melt}$) is close to that of the starting glass but displays a positive trend with temperature, increasing from +0.78 ± 0.04 ‰ at 660 °C to +1.10 ± 0.07 ‰ at 800 °C (Table 1). The low $\delta^{11}B$ value of DC-87 glass relative to starting glass may result from the occurrence of a fluid phase in this experiment because ^{11}B is expected to be preferentially partitioned into fluid relative to granitic melt (Maner and London, 2018). The B isotopic compositions of the experimental tourmaline ($\delta^{11}B_{Tur}$) show a positive correlation with temperature, increasing from −0.11 ± 0.04 ‰ at 660 °C to +0.86 ± 0.10 ‰ at 800 °C (Table 1). The calculated B isotope fractionation factors between melt and tourmaline ($\Delta^{11}B_{melt-Tur}$) increase from +0.23 ± 0.12 ‰ at 800 °C to +0.90 ± 0.05 ‰ at 660 °C (Table 1), and data regression indicates that the temperature dependence on $\Delta^{11}B_{melt-Tur}$ can be described as $\Delta^{11}B_{melt-Tur} = 4.51 \times (1000/T\ [K]) - 3.94$ ($R^2 = 0.96$) (Fig. 2a). In addition, the two experiments performed at 800 °C with different water activities (DC-27 and DC-28) show identical $\Delta^{11}B_{melt-Tur}$ values within uncertainties.

Discussion

Several lines of evidence suggest that near equilibrium conditions in terms of both major elements and B isotopes were reached between melt and tourmaline in our experiments: (1) microscopic observation shows that tourmaline is evenly distributed within the glass matrix for all experiments (Fig. 1a); (2) the major element compositions (seven to ten analytical points for each run) and B isotopic compositions (more than five analytical points) of experimental glasses from each experiment collected at different locations are identical within error (Tables S-2 and S-6); (3) apart from the hourglass sector zoning, no compositional zoning is observed in tourmaline; (4) no variation in B isotope composition is observed in experimental glasses next to the contact with tourmaline and far from the crystals (two or three points).

Our experimental data reveal a small and temperature-dependent B isotopic fractionation between granitic melt and tourmaline at magmatic temperatures. The degree of B isotopic fractionation between different phases at given *P-T* conditions is considered to be mainly controlled by the coordination of B in each phase, with trigonal site favouring ^{11}B and tetrahedral site favouring ^{10}B (Kowalski and Wunder, 2018). B in tourmaline is almost exclusively coordinated at the trigonal site ($^{[3]}B$); $^{[4]}B$ is expected in very Al-rich tourmaline (>1.2 atoms Al per formula unit at the Y site) and at high pressures (>1000 MPa) and low temperatures (Ertl *et al.*, 2018). Our experimental tourmaline is thus assumed to contain negligible amounts of tetrahedrally coordinated B. However, the $\delta^{11}B_{Tur}$ values show a systematic

Table 1 Experimental conditions and boron isotopic fractionation factors and partition coefficients.

Run[a]	B_2O_3 content (wt. %)[b]	*T* (°C)	*P* (kbar)	a_{H_2O}[c]	Duration (days)	Phases[d]	ASI[e]	$\Delta^{11}B_{melt}$ (‰)	s.d. (‰)	*n*	$\Delta^{11}B_{Tur}$ (‰)	s.d. (‰)	*n*	$\Delta^{11}B_{melt-Tur}$ (‰)	s.d. (‰)	*α*	1000ln*α*
DC-27	7.8	800	3	1.0	15	Tur (6.7), oxi (tr)	1.37	+1.10	0.07	5	+0.86	0.10	4	+0.23	0.12	1.0002	0.2308
DC-28	8.0	800	3	0.7	15	Tur (7.4), oxi (tr), fl	1.23	+1.10	0.02	5	+0.85	0.08	5	+0.25	0.09	1.0003	0.2559
DC-10	8.0	750	3	1.0	20	Tur (9), oxi (tr)	1.10	+0.96	0.08	6	+0.42	0.11	4	+0.54	0.13	1.0005	0.5459
DC-11	7.8	700	3	1.0	25	Tur (8.8)	1.20	+0.93	0.03	5	+0.31	0.11	4	+0.62	0.12	1.0006	0.6283
DC-87	7.7	660	3	1.0	30	Tur (10.8), oxi (tr), fl	1.24	+0.78	0.04	7	−0.11	0.04	4	+0.90	0.05	1.0009	0.9077

[a] Starting glass of all experiments was B10 glass.
[b] Boron contents of experimental glasses were measured by EMPA and calibrated based on data for synthesised glasses with different boron contents (B4, B6, and B10).
[c] Initial water activity in the experimental runs; $a_{H_2O} = H_2O/(H_2O + CO_2)$ on a molar basis.
[d] Numbers in parentheses represent phase abundances in wt. %, which were calculated by mass balance; tr, trace amount, but abundance not determined. Phase abbreviations: Tur, tourmaline; oxi, oxide; fl, fluid.
[e] Aluminum saturation index in the experimental glass; $ASI = Al_2O_3/(Na_2O + K_2O + CaO)$ on a molar basis.

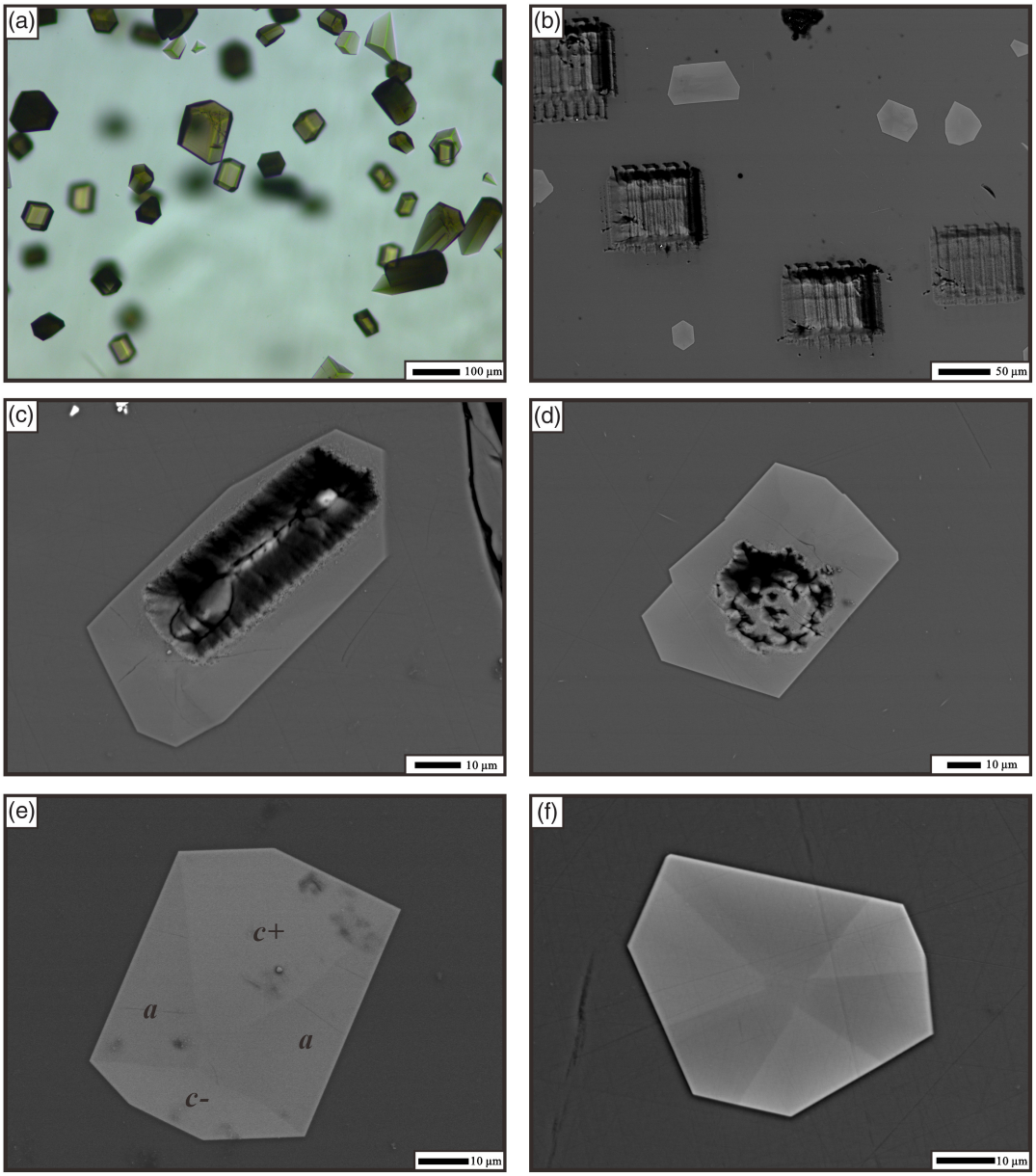

Figure 1 Representative images of experimental products. **(a)** Tourmaline is evenly distributed in melts (run DC-11, plane-polarised). **(b, c, d)** Representative BSE images of runs DC-10, DC-28, and DC-11, respectively, showing the positions of analysed areas with laser-ablation. **(e)** BSE image of a tourmaline grain with hourglass sector zoning from DC-87, section nearly parallel to the *c*-axis. Three zones can be recognised in this crystal: *c*+, *c*–, and *a* sectors (see details in SI). **(f)** BSE image of a tourmaline grain from DC-11 with hourglass sector zoning, section perpendicular to the *c*-axis. The image shows faceted compositional sector zoning splitting the crystal into light and dark areas.

increase with increasing temperature, which could be interpreted as a positive temperature effect on stabilising $^{[4]}$B at the T-site of tourmaline (Ertl *et al.*, 2018). In hydrous silicate glasses, B occupies both trigonally and tetrahedrally coordinated sites, and the proportions of $^{[3]}$B and $^{[4]}$B depend on melt composition (especially on B content), temperature, and pressure (Dingwell *et al.*, 1996). Previous spectroscopic measurements indicate that the amount of $^{[4]}$B in both natural and synthetic glasses is minor and probably negligible (Tonarini *et al.*, 2003). Since most B in magmatic tourmaline is at trigonal sites, the small $\Delta^{11}B_{melt–Tur}$ value implies that B should also be predominantly at 3-fold coordinated sites in the peraluminous B-rich granitic melts of this study. The slight increase in $\delta^{11}B_{melt}$ with increasing temperature in our experiments may be interpreted as the effect of temperature promoting the reaction $[BO_4] \rightarrow [BO_3] + NBO$ in silicate melts (Wu and Stebbins, 2013). It is noteworthy that some previous experimental studies observed a large B isotope fractionation between granitic melt and aqueous fluid, and interpreted it as an indication of a large proportion of $^{[4]}$B in the melt (Hervig *et al.*, 2002; Maner and London, 2018). This interpretation is inconsistent with both the result of this study and the spectroscopic studies.

This study provides a direct constraint on the B isotope fractionation between silicate melt and tourmaline and indicates a slightly positive value of $\Delta^{11}B_{melt–Tur}$. The $\Delta^{11}B_{melt–Tur}$ estimated from fluid-melt and fluid-tourmaline fractionation factors indicate a slight fractionation between granitic melt and tourmaline, but the sign of $\Delta^{11}B_{melt–Tur}$ is controversial (Fig. 2b). A $\Delta^{11}B_{melt–Tur}$ of −3 ‰ at 500 °C was applied by Trumbull *et al.* (2013) and Siegel *et al.* (2016), whereas Ribeiro da Costa

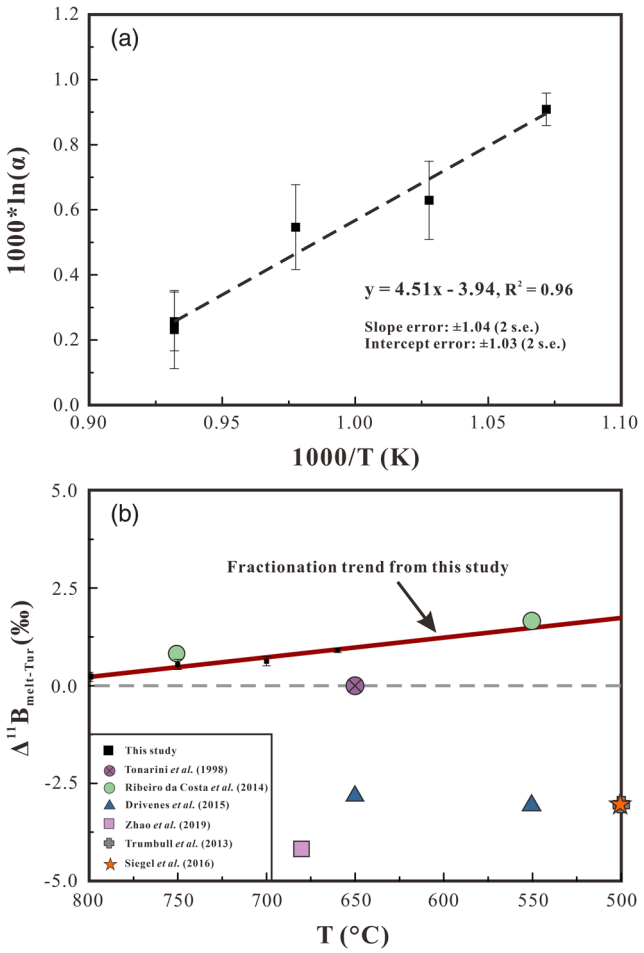

Figure 2 **(a)** Boron isotopic fractionation factors between granitic melt and tourmaline *versus* reciprocal temperature. The dashed line represents an Ordinary Least Square regression of the five fractionation values obtained from our experiments. **(b)** Comparison of $\Delta^{11}B_{melt-Tur}$ values from this study and $\Delta^{11}B_{melt-Tur}$ applied in previous studies to interpret $\delta^{11}B$ values analysed in tourmaline.

et al. (2014) used a positive factor to calculate the variation in B isotope composition of magma with tourmaline crystallisation. The inconsistency probably results from the difference in experimental and analytical methods as well as from different fluid compositions in the experimental studies on fluid-melt and fluid-tourmaline fractionation (Palmer *et al.*, 1992; Hervig *et al.*, 2002; Meyer *et al.*, 2008; Maner and London, 2018). Such problems could be overcome in this study. In addition, the composition of tourmaline formed in our experiments is similar to natural magmatic tourmaline (Figs. S-1 and S-2), which allows us to apply our results to granitic and pegmatitic systems.

Implications for Tracing Magma Evolution with Boron Isotopes

Boron isotope fractionation is expected to occur during magmatic–hydrothermal processes due to the difference in coordination of B between melt, fluid, and B-bearing minerals. As the most common B-rich mineral in granite and pegmatite, tourmaline is widely studied to trace processes at the magmatic–hydrothermal transition by measuring its B isotope composition. The results of this study show small slightly positive temperature-dependent $\Delta^{11}B_{melt-Tur}$ values. Thus, the B isotope composition of tourmaline crystallising from a granitic melt could approximately reflect that of the silicate melt, especially at high temperatures (~700–800 °C). However, since the residual melt will be progressively enriched in ^{11}B with ongoing crystallisation of tourmaline in a closed system, as indicated by the Rayleigh fractionation model (Fig. 3a), the $\delta^{11}B$ of late-magmatic tourmaline should be higher than that of tourmaline crystallising at an early stage. Such an increasing trend of $\delta^{11}B$ values from early- to late-stage tourmaline has been observed in pegmatite (Mikova *et al.*, 2010; Siegel *et al.*, 2016), based on the analysis of $\delta^{11}B$ in core and rim of tourmalines, reflecting the evolution from early- to late-stage crystallisation. Our calculation applying a Rayleigh fractionation model and the new fractionation factors show that the consumption of ~62–78 % B in melt (as a result of tourmaline crystallisation) could explain the observed B isotopic variation of tourmaline between core and rim (Fig. 3b). Differently, some other studies reported a decrease of $\delta^{11}B$ from early- to late-stage tourmaline in granites and pegmatites (Trumbull *et al.*, 2013; Drivenes *et al.*, 2015; Zhao *et al.*, 2019), which were ascribed to the preferential partitioning of ^{11}B in tourmaline relative to the coexisting melt because negative $\Delta^{11}B_{melt-Tur}$ values were assumed for the modelling (Fig. 3a, coloured lines). However, such an explanation is inconsistent with the positive $\Delta^{11}B_{melt-Tur}$ value determined in this study. Alternatively, a kinetically driven B isotope fractionation during fluid exsolution is a potential interpretation for the decrease of $\delta^{11}B$ observed in these studies (Kowalski and Wunder, 2018).

Conclusions

We determined the temperature-dependent equilibrium B isotope fractionation between peraluminous granitic melt and tourmaline at 660 to 800 °C and 300 MPa, which can be expressed as $\Delta^{11}B_{melt-Tur} = 4.51 \times (1000/T\,[K]) - 3.94$ ($R^2 = 0.96$). Our experiments, for the first time, provide direct measurements of the fractionation factors that can be used for tracing B isotopes of granitic melt from the records in tourmaline.

Acknowledgements

We thank U. Kroll, D. Qi, X. Li for their help of experiment and D. Wang for his assistance of EMPA analysis. The stay of L. Cheng at Hannover was supported by the Basic Research Fund of the Institute of Geology, China Earthquake Administration (IGCEA2018 and IGCEA1914). Laboratory costs were supported by the German Science Foundation (DFG, project HO1337/49). This paper has been greatly improved by the constructive comments from Horst R. Marschall, Vincent van Hinsberg, and an anonymous reviewer. We are also grateful to Horst R. Marschall for his editorial handling.

Editor: Horst R. Marschall

Additional Information

Supplementary Information accompanies this letter at https://www.geochemicalperspectivesletters.org/article2206.

© 2022 The Authors. This work is distributed under the Creative Commons Attribution Non-Commercial No-Derivatives 4.0 License, which permits unrestricted distribution provided the original author and source are credited. The material may not be adapted (remixed, transformed or built upon) or used for commercial purposes without written permission from the

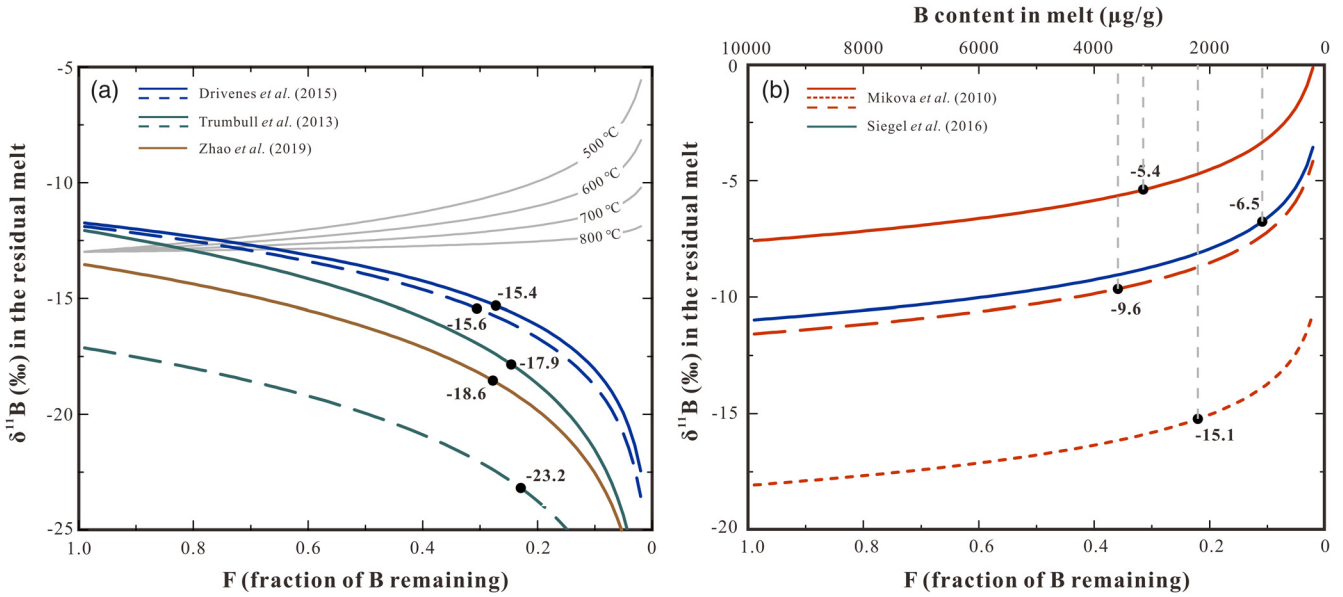

Figure 3 **(a)** Modelled curves illustrating the change in $\delta^{11}B$ values for residual melt after crystallisation of tourmaline, assuming a Rayleigh fractionation. Grey solid curves represent the evolution in $\delta^{11}B$ assuming tourmaline crystallisation, the starting $\delta^{11}B$ values of the melt are set as −13 ‰ and the fractionation factors are based on the result of this study. The coloured lines are calculated $\delta^{11}B$ variation trends of residual melts based on the $\delta^{11}B$ analyses of zoned tourmalines and negative $\Delta^{11}B_{melt-Tur}$ fractionation factors applied in the studies of Trumbull *et al.* (2013), Drivenes *et al.* (2015), and Zhao *et al.* (2019) (see data in Table S-8). Note the discrepancy between the grey solid lines and the coloured lines. **(b)** Rayleigh fractionation model illustrating the variation of $\delta^{11}B$ of residual melt with ongoing tourmaline crystallisation using tourmaline data from Mikova *et al.* (2010) and Siegel *et al.* (2016) and the positive fractionation factors from this study. The black dots in both figures represent $\delta^{11}B$ values of melt at the end of tourmaline crystallisation, calculated from the $\delta^{11}B$ values determined at the rim of the tourmalines. The $\delta^{11}B$ values at $F = 1.0$ are calculated from $\delta^{11}B$ values determined in the core of the tourmalines. Data used to draw the coloured lines are listed in Table S-8, and the detailed calculation process is given in SI.

author. Additional information is available at https://www.geochemicalperspectivesletters.org/copyright-and-permissions.

Cite this letter as: Cheng, L., Zhang, C., Zhou, Y., Horn, I., Weyer, S., Holtz, F. (2022) Experiments reveal enrichment of ^{11}B in granitic melt resulting from tourmaline crystallisation. *Geochem. Persp. Let.* 20, 37–42. https://doi.org/10.7185/geochemlet.2206

References

Dingwell, D.B., Pichavant, M., Holtz, F. (1996) Chapter 8. Experimental studies of boron in granitic melts. In: Anovitz, L.M., Grew, E.S. (Eds.) *Boron: Mineralogy, Petrology, and Geochemistry*. De Gruyter, Berlin, 331–385. https://doi.org/10.1515/9781501509223-010

Drivenes, K., Larsen, R., Müller, A., Sørensen, B., Wiedenbeck, M., Raanes, M. (2015) Late-magmatic immiscibility during batholith formation: assessment of B isotopes and trace elements in tourmaline from the Land's End granite, SW England. *Contributions to Mineralogy and Petrology* 169, 1–27. https://doi.org/10.1007/s00410-015-1151-6

Ertl, A., Henry, D.J., Tillmanns, E. (2018) Tetrahedral substitutions in tourmaline: a review. *European Journal of Mineralogy* 30, 465–470. https://doi.org/10.1127/ejm/2018/0030-2732

Hervig, R.L., Moore, G.M., Williams, L.B., Peacock, S.M., Holloway, J.R., Roggensack, K. (2002) Isotopic and elemental partitioning of boron between hydrous fluid and silicate melt. *American Mineralogist* 87, 769–774. https://doi.org/10.2138/am-2002-5-620

Kowalski, P.M., Wunder, B. (2018) Boron Isotope Fractionation Among Vapor–Liquids–Solids–Melts: Experiments and Atomistic Modeling. In: Marschall, H.R., Foster, G.L. (Eds.) *Boron isotopes*. Advances in Isotope Geochemistry. Springer, Cham, 33–69. https://doi.org/10.1007/978-3-319-64666-4_3

Li, Y.C., Chen, W.C., Wei, H.Z., Jiang, S.Y., Palmer, M.R., van de Ven, T.G.M., Hohl, S., Lu, J.J., Ma, J. (2020) Exploration of driving mechanisms of equilibrium boron isotope fractionation in tourmaline group minerals and fluid: A density functional theory study. *Chemical Geology* 536, 119466. https://doi.org/10.1016/j.chemgeo.2020.119466

London, D., Morgan, G.B., Wolf, M.B. (1996) Chapter 7. Boron in granitic rocks and their contact aureoles. In: Anovitz, L.M., Grew, E.S. (Eds.) *Boron: Mineralogy, Petrology, and Geochemistry*. De Gruyter, Berlin, 299–330. https://doi.org/10.1515/9781501509223-009

Maner, J.L., London, D. (2018) Fractionation of the isotopes of boron between granitic melt and aqueous solution at 700 °C and 800 °C (200 MPa). *Chemical Geology* 489, 16–27. https://doi.org/10.1016/j.chemgeo.2018.05.007

Marschall, H.R., Jiang, S.-Y. (2011) Tourmaline isotopes: no element left behind. *Elements* 7, 313–319. https://doi.org/10.2113/gselements.7.5.313

Meyer, C., Wunder, B., Meixner, A., Romer, R.L., Heinrich, W. (2008) Boron-isotope fractionation between tourmaline and fluid: an experimental re-investigation. *Contributions to Mineralogy and Petrology* 156, 259–267. https://doi.org/10.1007/s00410-008-0285-1

Mikova, J., Novák, M., Janousek, V. (2010) Boron isotopes in tourmalines of dravite–schorl series from granitic pegmatites of the Moldanubicum Zone, Czech Republic. *Acta Mineralogica-Petrographica Abstract Series* 6, 475.

Palmer, M.R., London, D., Morgan, G.B., Babb, H.A. (1992) Experimental determination of fractionation of $^{11}B/^{10}B$ between tourmaline and aqueous vapor: A temperature- and pressure-dependent isotopic system. *Chemical Geology: Isotope Geoscience section* 101, 123–129. https://doi.org/10.1016/0009-2541(92)90209-N

Ribeiro da Costa, I., Mourão, C., Récio, C., Guimarães, F., Antunes, I.M., Ramos, J.F., Barriga, F.J.A.S., Palmer, M.R., Milton, J.A. (2014) Tourmaline occurrences within the Penamacor-Monsanto granitic pluton and host-rocks (Central Portugal): genetic implications of crystal-chemical and isotopic features. *Contributions to Mineralogy and Petrology* 167, 1–23. https://doi.org/10.1007/s00410-014-0993-7

Siegel, K., Wagner, T., Trumbull, R.B., Jonsson, E., Matalin, G., Wälle, M., Heinrich, C.A. (2016) Stable isotope (B, H, O) and mineral-chemistry constraints on the magmatic to hydrothermal evolution of the Varuträsk rare-element pegmatite (Northern Sweden). *Chemical Geology* 421, 1–16. https://doi.org/10.1016/j.chemgeo.2015.11.025

Tonarini, S., Dini, A., Pezzotta, F., Leeman, W.P. (1998) Boron isotopic composition of zoned (schorl-elbaite) tourmalines, Mt. Capanne Li-Cs pegmatites, Elba (Italy). *European Journal of Mineralogy* 10, 941–951. https://doi.org/10.1127/ejm/10/5/0941

Tonarini, S., Forte, C., Petrini, R., Ferrara, G. (2003) Melt/biotite $^{11}B/^{10}B$ isotopic fractionation and the boron local environment in the structure of volcanic

glasses. *Geochimica et Cosmochimica Acta* 67, 1863–1873. https://doi.org/10.1016/S0016-7037(02)00987-0

Trumbull, R.B., Beurlen, H., Wiedenbeck, M., Soares, D.R. (2013) The diversity of B-isotope variations in tourmaline from rare-element pegmatites in the Borborema Province of Brazil. *Chemical Geology* 352, 47–62. https://doi.org/10.1016/j.chemgeo.2013.05.021

Wu, J., Stebbins, J.F. (2013) Temperature and modifier cation field strength effects on aluminoborosilicate glass network structure. *Journal of Non-Crystalline Solids* 362, 73–81. https://doi.org/10.1016/j.jnoncrysol.2012.11.005

Zhao, H.D., Zhao, K.D., Palmer, M.R., Jiang, S.Y. (2019) In-situ elemental and boron isotopic variations of tourmaline from the Sanfang granite, South China: Insights into magmatic-hydrothermal evolution. *Chemical Geology* 504, 190–204. https://doi.org/10.1016/j.chemgeo.2018.11.013